...TION OF SATURATION MAGNETISATION, ...PERATURE AND LATTICE PARAMETER OF Ni.$_3$ Zn.$_7$ Fe$_2$ O$_4$

By

V. S. ANANTHAN

...PARTMENT OF METALLURGICAL ENGINEERING

...INSTITUTE OF TECHNOLOGY KANPUR

AUGUST, 1983

OF $Ni._3 Zn._7 Fe_2 O_4$

A Thesis Submitted
In Partial Fulfilment of the Requirements
for the Degree of
MASTER OF TECHNOLOGY

By

V. S. ANANTHAN

to the
DEPARTMENT OF METALLURGICAL ENGINEERING
NDIAN INSTITUTE OF TECHNOLOGY KANPUR
AUGUST, 1983
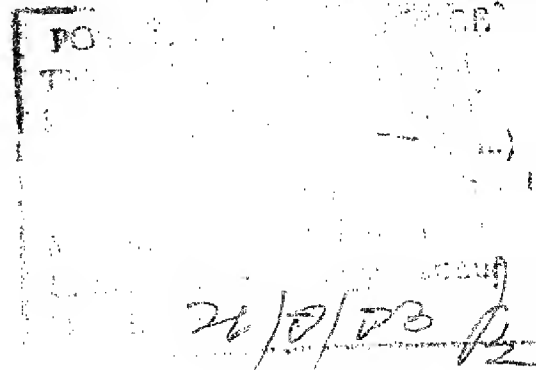
CERTIFICATE

Certified that the thesis entitled, 'EFFECT OF TITA

ZIRCONIUM AND TIN ON THE VARIATION OF SATURATION MAGNETI

CURIE TEMPERATURE AND LATTICE PARAMETER OF $Ni_{.3}Zn_{.7}Fe_2O_4$

FERRITE' has been carried out under our supervision and

has not been submitted elsewhere for a degree.

(Dr. D.C. Khan)　　　　　　　　(Dr. A.R. Das)
　Professor　　　　　　　　　　　　Professor
Department of Physics　　　Department of Mett. Engg.
　I.I.T. Kanpur.　　　　　　　　I.I.T. Kanpur.

LIST OF TABLES

LIST OF FIGURES

CONTENTS

ACKNOWLEDGEMENTS

I express my hearty gratitude to Dr. A.R. Das for his able guidance and constant help throughout the course of this work.

I owe my sincere gratitude to Dr. D.C. Khan for his valuable suggestions and guidance throughout the course of the work.

I thank Dr. Misra for his interest in the problems and for providing the computer program.

I thank Mr. R.K. Prasad and Mr. Malvia of Ceramics Lab. for their extensive help throughout the works. I also thank Mr. Chaurasia of Analytical Chemistry, Mr. Mongle of Thermodynamics lab., Mr. Agnihotri and Mr. Jain of ACMS for their help.

My thanks are due to Mr. S. Balaram for his assistance and to all other friends who helped me in some way or other.

V.S. ANANTHAN

CHAPTER 1

INTRODUCTION

The outstanding feature of ferrites as magnetic
materials is their high resistivity which makes them
particularly suitable for applications in high frequency
systems where its high resistivity ensures low losses. The
ferrite industry was established about thirty-five years ago
following the classical investigations of J.L. Snoek[1].

Ferrites are oxides with a formula $MeOFe_2O_3$, where
Me represents divalent cations like Mn,Fe,Co,Ni,Cu,Zn etc.,
and has an inverse spinel structure. Oxygen with relatively
larger radii form an face centered cubic lattice. In this
closed packed structure two kinds of interstitial sites
occur, the tetrahedral (A) and octahedral (B), sites which
are surrounded by 4 and 6 oxygen ions respectively. A unit
cell has 32 O^{2-} ions with 64 tetrahedral and 32 octahedral
sites. The metal ions having radii $0.4 - 1.0$ $\overline{A}$ are distri-
buted amongst these sites.

The distribution of cations at A and B interstices
give rise to three type of spinel structures :
(1) 'Normal spinel' in which Me occupies the tetrahedral
      position and Fe^{3+} in the octahedral position and is
      written as $Me\ [Fe_2]O_4$.

(2) 'Inverse spinel' in which Me occupies the octahedral position together with half of Fe^{3+} while the other half Fe^{3+} occupies the tetrahedral position and is written as $Fe[MeFe]O_4$.

(3) 'Intermediate spinel' as $Fe_{1-x}Me_x[Me_{1-x}Fe_{1+x}]O_4$.

The distribution of cations amongst these sites based on crystal field theory was explained by Gorter[2]. According to this theory, the magnetic interaction (super-exchange) energy is strongly dependant on the distribution of magnetic ions amongst the crystallographic positions. The influence diameter and charge of a cation on its preference to A or B site in an oxidic spinel is not an individual property as the diameter and charge of other cations must be taken into account.

Later, Blasse[3] deduced the site preference energy qualitatively using Ligand field theory. Ligand field theory is the use of molecular orbitals and introduces partly covalent bonding and crystal field stabilization simultaneously. The results obtained are more reliable than those due to crystal field theory.

Ni^{2+} has a strong preference for 6-fold co-ordination and Zn^{2+} for 4-fold co-ordination. The preference of zinc to A site is utilised to improve the property of nickel ferrite. The addition of Zn^{2+} ions to nickel ferrite forces

Fe^{3+} ions from A to B sites. This should give an additio[n]
magnetisation of B-sites. However, Gorter[2] found that i[t]
does not increase. The addition of more than 50 mole per[cent]
of zinc in nickel ferrite reduces the net magnetic momen[t]
from the peak value as the reduced number of Fe^{3+} ions i[n A]
sites becomes less able to maintain the alignment of B
sublattice moments against BB interaction. The curie
temperature (T_c) decreases linearly with increase of zinc
content.

The variation of saturation moment, curie temperatu[re]
and susceptability of ferrimagnetic compounds as a result
of substitution of nonmagnetic ions in place of magnetic
ions can be understood to a good approximation on the
basis of random distribution of incomplete superexchange
interactions. Gilleo[4] has derived expressions for satura-
tion magnetisation and curie temperature based on super-
exchange interaction of magnetic ions of different co-
ordination. Using Gilleo's formula, curie temperature
for $Cu_x Zn_{1-x} Fe_2O_4$ samples were evaluated by Swant et a[l]

The exchange interactions between magnetic ions in A
and B sites govern the magnetic ordering temperature (T_c)
The interaction energy between a magnetic moment 'S_i' on
site 'i' and 'S_j' on site 'j' is given by the expression

$$E_{exchange} = -2J_{ij} S_i S_j$$

where J_{ij} is the exchange constant which depends on the distance between magnetic ions and the symmetry of local arrangement of anions and cations. The various interactions possible in a spinel are AA, BB and AB interactions.

Bongers et al.[6] studied the curie temperature variation as a function of Fe^{3+} on A and B sites for Rh, Ti and Sb substituted $MgFe_2O_4$ and calculated $J_{AB}(Fe^{3+}-Fe^{3+})$ using the slope of the curve. He was also able to account this temperature variation on the basis of strong BB interaction

The exchange constants for titanium substituted $Ni_3 Zn_{.7} Fe_2O_4$ system using 3-sublattice Yafet-Kittel type model of Satayamurthy et al.[7], was calculated by Misra[8] and found the results agreeable with those of Sreevastava et al.[9].

Gorter[2] reported that the effect of Ti^{4+} ion in an inverse spinel ferrite is to replace the ferric ion completely or partly thereby reducing the saturation moment. He had worked on the effect of Ti^{4+} ion on nickel ferrite and nickel zinc ferrite where the titanium ion occupies the octahedral sites only.

According to J.E. Knowles[10] the effect of Ti^{4+} ion in Mn-Zn ferrite is to localize ferric ion which increases resistivity and reduces loss. The anomalous results when

tin ion. When ferrite is cooled down from high temperature the quatrivalent ions tend to migrate to the preferred B sites which is facilitated by the presence of cation vacancies. During this process upto 1/3 of larger tin ion gets 'frozen in' in A site thereby increasing the magnetisation. But the replacement of Ti^{4+} ion by Sn^{4+} ion lowers curie temperature (T_c). The lattice parameter is also found to increase with tin content.

Stinges et al.[11] found the substitution of T_i^{4+} in Mn-Zn ferrite takes place on octahedral sites by replacing $2Fe^{3+}$ by $Fe^{2+}+Ti^{4+}$ under reducing conditions, which increases magnetic anisotropy. The lowering of curie temperature with titanium addition was found to be very small. He had also studied the variation of saturation magnetisation (M_s) with titanium addition.

For $Ni_{1-x} Zn_x Fe_2O_4$ as x value decreases the material becomes magnetically softer to harder. In soft ferrite as in our $Ni_{.3} Zn_{.7} Fe_2O_4$, the internal magnetic forces are relatively small, implying that anisotropy is small and domain walls movement are easier. Thus the magnetic spins yield easily to external field giving high permeability. The coercivity is small and the curie point is low.

The properties of ferrites depend on microstructure and chemical composition. The effect of processing parameters on the microstructure development of $Ni_{.3} Zn_{.7} Fe_2O_4$ ferrite is discussed by Gupta[12]. The properties are sensitive to stoichiometry[13]. Sintering of such ferrites are carried out at $1100-1250^{\circ}C$. High sintering temperature leads to dense product. Slick and Blassches[14] noted sublimation of zinc oxide in Mn-Zn ferrite as a result of decrease of oxygen content or increase of sintering temperature. The partial pressure of zinc is maintained by the use of packing material while firing thereby avoiding the loss of zinc from the system.

V.V. Pankov et al.[15] have worked on the mechanism of Ni-Zn ferrite formation. They have shown that the reaction zone of interacting NiO, ZnO with Fe_2O_3, the ferrite phase crystallizes on iron oxide. Also, the interaction of (Ni,Zn)O solid solution with Fe_2O_3 takes place by the mechanism Fe^{3+}, Fe^{2+} and Ni^{2+}, Zn^{2+} ion interdiffusion and have applied Wagner-model to determine the reaction rate constant.

Miter T. Dimova[16] found that in Ni-Zn ferrite the concentration of free Fe_2O_3 was 1/3 to 1/2 after double ferriti sation compared to the single process under same conditions.

The lattice constant of the whole range of $Ni_x Zn_{1-x} Fe_2O_4$

A.S.T.M[18]. The variation of saturation magnetisation with temperature for some ferrites of $Ni_{1-\delta} Zn_{\delta} Fe_2O_4$ series are given in Smit and Wijn[19]. The saturation magnetisation, an important property of soft ferrites, was extensively studied by Gorter[2] and brought out a clear picture in the magnetic saturation moment between theoretical and practical values.

AIM OF THE PROBLEM

High-valent non-magnetic cations when substituted in ferrite are expected to create vacancies under oxidising conditions. This should result in a monotonic variation of lattice parameter, saturation magnetisation and curie temperature. However, a sharp initial dip and subsequent rise in the lattice parameter, curie temperature and saturation magnetisation was observed in case of titanium substituted Ni-Zn ferrit by earlier workers[8,25]. Similar behaviour of magnetic moment in other high-valent substitutions was also observed[25]. The samples prepared by the above workers were by solid-state reaction and the chemical homogenity of the final material were thought to be insufficient.

Hence, it was decided to add high-valent dopants such as titanium, zirconium and tin by solution method to $Ni_{.3}Zn_{.7}Fe_2O$ and verify the following parameters.

1) Variation of lattice parameters,

2) Variation of saturation magnetic moment, and

3)   Curie temperature variation with the addition of the
      dopants.

The dopants Ti^{4+}, Zr^{4+} and Sn^{4+} have ionic radii close
to that of Ni^{2+}, Zn^{2+} and Fe^{3+} so that they can substitute ions
from base Ni-Zn ferrite.

EXPERIMENTAL METHOD

3.1 RAW MATERIALS

The raw materials used for preparation of Ni-Zn-ferrite and corresponding dopants are given below.

Raw materials	Grade
a) Nickel metal (Ni)	> 99%
b) Zinc metal (Zn)	> 99%
c) Iron metal (Fe)	Crystal bar grade > 99.5%
d) Titanium metal (Ti)	Crystal bar grade > 99.5%
e) Zirconium metal (Zr)	Crystal bar grade > 99.5%
f) Tin metal (Sn)	> 99%
g) Sulphuric acid (H_2SO_4)	A.R.
h) Nitric acid (HNO_3)	A.R.
i) Hydrofluoric acid (HF)	L.R.

For packing material iron oxide, nickel oxide and zinc oxide of L.R. grade are used.

3.2 PREPARATION OF THE PACKING MATERIAL

The nickel oxide, zinc oxide and iron oxide powders were weighed accurately in an electronic pan balance

(Osbar, Germany) following Table 2. Hand pellets were made with 5 percent PVA (polyvinyl alcohol) as the binder. The pellets were fired directly in an electrically heated silicon-carbide furnace at $1200^{\circ}C$ for 6 hours in sillimanite crucibles. After firing, the pellets were ground in an agate mortar to fine powder (-50 mesh).

3.3 PREPARATION OF SAMPLES

3.3.1 Preparation of base solution

Nickel : The nickel metal powder was weighed accurately as in Table 2. The metal was dissolved in hot concentrated nitric acid. The required amount of the solution was made up

Zinc : The zinc metal was cut into small pieces with diamond wheel cutter and weighed accurately. It was then reacted with hot concentrated sulphuric acid. The zinc sulphate formed was slowly dissolved in distilled water by constant stirring and slow heating. The required amount of solution was prepared.

Iron : The weighed amount of iron was dissolved in 50 percen concentrated nitric acid and the required amount of solution was prepared.

3.3.2 Mixing of the base solution

The base solutions of nickel, zinc and iron containing their respective salts were then thoroughly mixed to give

a clear solutions. The amount of solution prepared was noted and the strength was calculated.

3.4 PREPARATION OF DOPANT SOLUTIONS

Titanium : Known amount of titanium (Table 3) was taken in a platinum crucible and hydrofluoric acid was added. It was gently heated to completely dissolve the metal. The solution was then added to a beaker containing sulphuric acid and a predetermined amount of solution was prepared.

Zirconium : In a similar manner as titanium, zirconium was treated with hydrofluoric acid for 6 to 8 hours to completely dissolve the metal. This solution was then added to sulphuric acid to prepare the standard solution.

Tin : Tin was heated in concentrated sulphuric acid when the metal was completely dissolved and a predetermined amount of solution was prepared.

3.5 ADDITION OF DOPANT SOLUTIONS

The exact volume of dopant solutions required for adding to the base solution in order to get the required weight percentages of the dopants were calculated. The calculated volumes of the dopant solutions were added to the base solution slowly with uniform stirring.

Dopant-added solutions of different percentages were separately prepared as shown in Table 3.

3.6 DRYING OF THE MIXTURE OF SOLUTIONS

The solutions prepared as above were then heated to dryness in an oven kept in the fuming chamber. The heating time was about 4 to 5 hours.

3.7 THERMAL DECOMPOSITION

The dried salts were than transferred to alumina crucibles. Then they were heated in an electric furnace a $800^{o}C$ for 4 hours. At this temperature the decomposition of all the salts present takes place to form the corresponding oxides. A fine mixture of oxides was got in correct propositions of weight.

3.8 HEAT TREATMENT

The decomposed sample in the form of fine powder was ground in an agate mortar to yield a thorough mixture. With the use of small amount of PVA as the binder, pellets were hand formed. These pellets were covered with packing material and fired at $1200^{o}C$ for 2 hours.

After cooling, the samples were reground to fine powder. Small pellets of 3 mm diameter were made in a small punch and dye with the help of PVA as binder. The remaining sample was again hand formed with the same binder. The pellets were refired at $1200^{o}C$ for 4 hours in alumina crucibles.

After cooling, the hand formed samples were ground to fine powder (-50 mesh) for x-ray studies. The 3 mm diamt pellets were used for magnetic studies.

Throughout the firing operation, the temperature of t furnace was controlled carefully by the use of on-off con- troller (Leeds and Northrup, Electromax). A temperature profile of the heating muffle was drawn with the help of Platinium-Platinum 10 percent Rhodium thermocouple to locate the region of desired temperature.

3.9 X-RAY ANALYSIS

3.9.1 Optimising the ferritisation temperature

The base $Ni_{.3} Zn_{.7} Fe_2O_4$ sample powder was studied in Seifert X-ray diffractometer (Germany) with chromium as target. X-ray diffractograms were taken for samples fired at different temperatures and the data were compared with ASTM data of the NiO, ZnO and Fe_2O_3 and for the final product.

3.9.2 Characterisation of Ni-Zn ferrite

The X-ray diffractogram of the base sample was taken and the d-spacing was compared with ASTM data for Ni-Zn ferrite.

3.9.3 Step scan analysis

The shift in d-values for different dopants at various weight percentages can be found out only by noting

the exact peak positions. This was done by the use of automatic step scan available in Seifert X-ray diffractometer.

First by knowing the approximate peak positions, the sample was set about 0.5 degree less than the maximum peak position. The angles were then changed by steps of 0.05 degrees and the number of counts for ten seconds at each step were printed automatically. The counts were plotted against the angle to determine the exact peak position. This was repeated for all peaks and samples.

3.9.4 Lattice Parameter Calculations

The measured angle (2θ) values and the wavelength of chromium target used were given as data in the computer program for calculating the d value and the corresponding lattice parameter. The lattice parameter values were plotted against the Nelson-Riley function $f(\theta)$. The curve of $f(\theta)$ versus the lattice parameter (a) is expected to be a straight line and the extrapolated 'a' corresponds to $f(\theta) = 0$, using the least square fit gives accurate value of 'a' (Refer Appendix).

3.10 MAGNETIC MEASUREMENTS

3.10.1 Saturation magnetisation

The samples were prepared for magnetic studies as in Section 3.8. The pellets were weighed accurately. The

samples were then tested in the magnetic field of a parallel field vibrating magnetometer (PARC model 150A). In this magnetometer, the samples are kept at vibration in vertical direction and the magnetic field applied acts horizontally. The magnet is capable of producing a maximum field of 10 K Oe with a pole gap of 2.5 inches. The induced a.c field produced by the sample in a pair of secondary coils placed on both sides of the sample is amplified and compared with the signal produced by a standard magnet giving rise to an output signal which is proportional to the magnetic moment of the sample.

The magnetic field was applied gradually in steps upto 10 KOe, and the saturation moment of all samples at this field were taken at room temperature.

The saturation moment is given by

$$\sigma = \sigma_0/m \ (emu/gm\ ) \quad or\ by\ 4\pi M_s (gauss)$$

where σ_0 is the observed magnetic moment, m is the mass of the sample, and M_s is given by $M_s = \sigma\ x$, (—density gms/cc).

3.10.2 Curie temperature

The variation of magnetic moment with temperature at residual field of 40 Oe were observed for all the samples. The temperature of the samples were measured by NiCr-NiAl thermocouple. The heating rate of the samples were slow and

uniform. Near the expected value of curie temperature (T_c), the magnetic moment variation at very small (2-5 degree centigrade) were noted. Then $\frac{d\sigma}{dT}$ versus T curves were plotted using interpolation techniques. The ferromagnetic transition temperature (T_c) is defined as that temperature at which $\frac{d\sigma}{dT}$ versus T curve shows a minimum.

RESULTS

4.1 RAW MATERIALS

The samples and the packing material were prepared in accordance with the compositions given in Tables 2 and 3. About 10-15 grams of batch of sample and 500 grams of packing material were prepared.

4.2 PREPARATION OF PACKING MATERIAL

A ferritised powder was obtained when the raw materials were fired at $1200^{\circ}C$ for 6 hours. The composition was chosen similar to the basic $Ni_{.3}Zn_{.7}Fe_2O_4$ ferrite.

Zinc has a low vapour pressure and sublimates at high temperatures. To prevent the expulsion of zinc from the sample during firing, proper oxygen partial pressure was provided by covering the samples with packing material. Pure zinc-oxide was not used as the packing material to avoid the diffusion of zinc from the highly concentrated packing zone into the sample.

4.3 PREPARATION OF SAMPLES

4.3.1 Preparation of base-solutions

Nickel : The nickel metal was readily dissolved in hot concentrated nitric acid to form nickel nitrate. The

nickel nitrate formed decomposes to nickel oxide before it becomes anhydrous[20] as

$$2Ni(NO_3)_2 = 2NiO + 4NO_2 + O_2$$
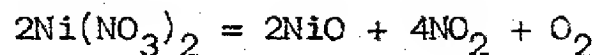
Zinc : Zinc metal forms zinc sulphate on heating with concentrated sulphuric acid. Zinc sulphate decomposes at $600^\circ C$ to form zinc oxide[21].

Iron : The iron metal was dissolved in nitric acid with slight heating. Iron nitrate decomposes to iron oxide on heating[22] as

$$Fe + 2HNO_3 = Fe_2(NO_3)_2 + H_2$$

$$6Fe(NO_3)_2 + 5H_2O = 3Fe_2O_3 + (2NO+10HNO_3)$$
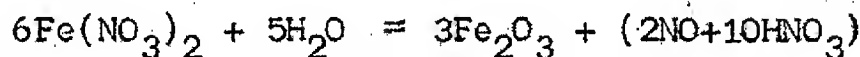
4.3.2 Mixing of the base-solutions

The mixture of solutions containing the salts of iron, nickel and zinc was clear and homogenous.

4.4   Preparation of dopant solutions

The dopants were dissolved in acid and then added to the base-solution. This was done to improve the homogenity of the dopants with the basic Ni-Zn ferrite.

Titanium and zirconium did not dissolve in sulphuric acid as the metals were not in the powdered form. So these metals were initially dissolved in hydrofluoric acid and further treated with sulphuric acid to form the corresponding metal sulphates[23,24]. The solutions were gently heated to evaporate the hydrofluoric acid. The evaporation of hydrofluoric acid was observed as white fumes. The titanium and zirconium sulphates decompose at $708^{\circ}C$ and $798^{\circ}C$ respectively[25]. Tin dissolved readily in sulphuric acid to form tin sulphate which decomposes to tin oxide on heating.

4.5 ADDITION OF DOPANT SOLUTIONS

The amount of dopant solutions added to the base-solution was in accordance to Table 3. The solutions were added using a micro-burette which reads upto 0.05 ml.

4.6 DRYING

The solutions when dried gave a mixture of salts containing iron, nickel, zinc and dopants in proper pro-positions.

4.7 THERMAL DECOMPOSITION

The salts of various elements present after drying were thermally decomposed to form their corresponding oxides. The complete decomposition was verified by their weight loss. The oxides were obtained in the form of fine particles.

4.8 HEAT TREATMENT

The initial grinding of the metal oxides improved the homogenity. The handformed pellets were made to improve ferritisation rate. The use of packing material avoided zinc escaping from the system.

After initial firing at $1200^{\circ}C$, the material was reground thereby further improving the homogenity of the metal oxides. Completely ferritised sample was obtained after refiring at $1200^{\circ}C$ for 4 hours.

4.9 X-RAY ANALYSIS

4.9.1 Optimising the ferritisation temperature

The X-ray diffractograms were taken for all $Ni_{.3}Zn_{.7}Fe_2O_4$ samples fired at different temperatures, ranging from 1000 to $1150^{\circ}C$. The ferritisation was complete at $1150^{\circ}C$. This was indicated by the peaks in the diffractogram when they were identified with that of the final product. The firing temperature was chosen $50^{\circ}C$ above the required temperature to ensure complete ferritisation.

4.9.2 Characterisation of Ni-Zn ferrite

The result of the X-ray diffraction lines of base $Ni_{.3}Zn_{.7}Fe_2O_4$ is given in Table 4. The d-spacings were compared with the ASTM data for Ni-Zn ferrite. The hkl

indices were adopted from the ASTM data. The (311) planes refer to the maximum observed intensity.

4.9.3 Step scan analysis

The counts of the peaks in steps of 0.05 degree were taken. The angle (2θ) versus the counts were plotted and the curves in all the cases were smooth. Hence, the exact 2θ value was determined as given in Appendix.

4.9.4 Lattice parameter

Accurate determination of lattice parameter is discussed in Appendix. The results of estimated d, hkl, lattice parameter and the corresponding Nelson-Riley functions are indicated in Tables 5,6 and 7. The extrapolated values of lattice parameter of all the samples are given in Tables 5,6,7 and 9.

Figure 1 shows the variation of lattice parameter with the addition of titanium, zirconium and tin in $Ni_{.3}Zn_{.7}Fe_2O_4$.
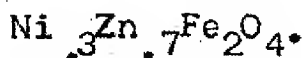
It is observed for very small additions of titanium the lattice parameter decreases and for 0.5 wt% and above the lattice parameter increases. The dip is found minimum at 0.25 wt% of titanium when the lattice parameter decreases from 8.4178$\overline{A}$ to 8.4127$\overline{A}$. This is followed by a continuous increase at higher percentages as seen in Figure 1.

In case of zirconium addition (Figure 1) the lattice parameter increases upto 1 wt % and then it tends to flat upto 1.5 wt % . The solubility of zirconium is limited above 1 wt % . The peaks of monoclinic ZrO_2 were observed at 3 and 8 wt % . The amount of ZrO_2 entering the spinel lattice is not calculated at these weight percentages.

In case of tin the solid solubility is observed upto 5 wt % , the limit of this study. The lattice parameter increases monotonically for all weight percent addition of the dopant.

4.10 MAGNETIC MEASUREMENTS

4.10.1 Saturation magnetisation

The variation of magnetic moment with the applied field for base $Ni_{.3}Zn_{.7}Fe_2O_4$ at room temperature is given in Table 8 and illustrated in Figure 2. The maximum field applied is 10KOe. The variation of saturation magnetic moment at room temperature with the addition of the dopant is given in Table 9 and Figures 7,8 and 9.

In case of titanium addition the magnetic moment falls steeply at low percentages followed by an increase a again falls to low values at higher percentages as seen in Figure 7. The minimum moment of the initial dip is at 0.5 wt % of titanium addition.

With 0.25 wt % of zirconium addition the magnetic moment falls steeply from the initial value. Upto 1 wt % the moment decreases by a small amount and above 1 wt % it increases by a small amount (Figure 8). The initial steep decrease of moment is found in tin additions upto 0.5 wt %. Further additions upto 5 wt % reduces the moment continuously by a small amount as shown in Figure 9.

4.10.2 Curie temperature

The variation of magnetic moment at residual field (40 Oe) with temperature was studied for $Ni_{.3}Zn_{.7}Fe_2O_4$ after 2,4 and 6 hours of firing duration. The samples were reground after each firing and the nature of the curve improved significantly with increased firing duration. The samples after 6 hours of firing shows a relatively sharper transition as seen in Figure 3.

In Figures 4,5 and 6 the temperature variation of the magnetic moment at residual field (40 Oe) for titanium, zirconium and tin additions is shown. The curie temperatures (T_c) of all samples were determined with the help of a computer program (provided by Dr. M. Misra) involving spline interpolation technique. The curie temperature of base $Ni_{.3}Zn_{.7}Fe_2O_4$ was compared with Misra[8] and they match very well. Table 9 shows the curie temperature calculated for all samples doped with titanium, zirconium and tin.

Figure 7 shows the variation of curie temperature with the addition of titanium in $Ni_{.3}Zn_{.7}Fe_2O_4$. The transition temperature (T_c) initially falls steeply and shows a minimum at 0.5 wt % . This is followed by an increase upto 1.5 wt % when again it starts lowering at 3 and 8 wt % . The trend of this curve is similar to that of the magnetic moment variation curve (Figure 7). Similar dip is found in zirconium additions with minimum T_c at 0.25 wt % (Figure 8). Two dips are found for tin additions at 0.25 and 1 wt % as shown in Figure 9. In both zirconium and tin additions the dips are not as prominent as in titanium.

DISCUSSION

SATURATION MAGNETISATION

The present observations of variation of magnetic
nt when high valent cations such as titanium, zirconium
tin substituted $Ni_{.3}Zn_{.7}Fe_2O_4$ are the following :

There is a steep fall of initial magnetic moment
in all three additions.

The initial steep fall is followed by a subsequent
rise and fall in magnetic moment in the case of titan
addition (Fig. 7).

The initial steep fall is followed by a small rise in
magnetic moment in the case of zirconium addition
(Fig. 8).

The initial dip is followed by a gradual decrease of
magnetic moment in the case of tin addition (Fig. 9).

The dip in magnetic moment when similar high valent
ons were substituted in Ni-Zn ferrite was observed by
ier workers[8,26,27]. The observed phenomenon of sharp
ease of magnetic moment is quite contrary to the expec
tonic decrease when high valent non-magnetic ions are
tituted in Ni-Zn ferrite.

Possible explanations were given by earlier workers[26,27,8]to this observed dip in the magnetic mo Das[26] presumed the variation of magnetic moment with addition of all non-magnetic ions to behave in a sim manner as the addition of zinc around the compositio point. The variation was arbitrarily taken from sat tion magnetisation (M_s) versus zinc content curve (Gorter[2]) and calculated the variation of M_s in tita substituted $Ni_{.5}Zn_{.5}Fe_2O_4$ based on Yafet-Kittel[28] re ship as,

$$M_s = M_b \sin\varphi - M_a,$$

where M_b and M_a are the saturation magnetisation of sublattices and $(\pi-2\varphi)$ is the canting angle of the s components of B. The calculation of the slope $\frac{dM_s}{dx}\Big|$

where x is the amount of dopant added was shown to b negative both for A or B site substitution of titani with slopes being different.

On the same basis Sen[27] calculated the slope o magnetic moment with titanium addition in $Ni_{.3}Zn_{.7}Fe$ and showed negative slopes in A or B substitutions. was no explanation given by the above workers for t subsequent rise in the magnetic moment. But in both cases a larger negative slope was seen in A site occ

Possible explanations were given by earlier workers[26,27,8] to this observed dip in the magnetic mo Das[26] presumed the variation of magnetic moment with addition of all non-magnetic ions to behave in a sim manner as the addition of zinc around the compositio point. The variation was arbitrarily taken from sat tion magnetisation (M_s) versus zinc content curve (Gorter[2]) and calculated the variation of M_s in tita substituted $Ni_{.5}Zn_{.5}Fe_2O_4$ based on Yafet-Kittel[28] re ship as,

$$M_s = M_b \sin\varphi - M_a,$$

where M_b and M_a are the saturation magnetisation of sublattices and $(\pi-2\varphi)$ is the canting angle of the s components of B. The calculation of the slope $\left.\dfrac{dM_s}{dx}\right|$

where x is the amount of dopant added was shown to b negative both for A or B site substitution of titani with slopes being different.

On the same basis Sen[27] calculated the slope o magnetic moment with titanium addition in $Ni_{.3}Zn_{.7}Fe$ and showed negative slopes in A or B substitutions. was no explanation given by the above workers for t subsequent rise in the magnetic moment. But in both cases a larger negative slope was seen in A site occ

than for B site. In case of Das the slope was 1.6 times higher for A site occupancy and it was 5.7 times in the case of Sen. This difference may be due to two different compositions of the ferrite and hence two different canting angles.

The analysis of cation distribution and calculation of saturation magnetisation by Misra[8] based on Satyamurthy's 3-sublattice model gives a better reasoning for the observed phenomenon. In the three sublattice model of ferrimagnetism the B sublattice is divided into B_1 and B_2 each of which is oriented at an angle $(\pi-\varphi)$ in opposite direction with respec to the moment of A sublattice where φ is the Yafet-Kittel angle. He had calculated the canting angle for different additions of titanium from the interaction parameters of different cations which enabled him to calculate the cation distribution of titanium substituted $Ni_{.3}Zn_{.7}Fe_2O_4$.

Based on Misra's model, for small concentrations of titanium ions, the substituting ion enters the A site only. After a critical value of concentration it starts entering B site and at higher concentrations it enter A and B sites with equal preference.

His model of $Ti^{4+} \rightarrow Fe^{3+} + \frac{1}{2} (Ni_{.3}Zn_{.7})^{2+}$ resulting in half vacancy of divalent cation and Ti^{4+} going to A site together with some transfer of Fe^{3+} from A to B site account.

for the initial dip. After a critical composition, Ti^{4+} enters B site resulting in a transfer of Fe^{3+} from B to A site, thereby increasing the magnetic moment. At higher percentages Ti^{4+} enters both A and B sites and the transfer process of Fe^{3+} is reduced to a low value. Similar analysis like Misra could not be carried out in the present work as the interaction parameters and the canting angle were not calculated. This restricted us in determining the cation distribution and hence the theoretical magnetic moment

Misra's model may qualitatively explain the behaviour of M_s variation with dopant addition in the case of zirconium which shows a sharp initial fall followed by a small rise though this dip and subsequent rise is accentuated in the case of titanium. In the case of tin the initial steep fall is followed by a gradual slope of the curve.

This model is unable to explain the sharp initial dip in magnetic moment of 29.76 percent per $\frac{1}{2}$ wt % of titanium addition in Misra's observation and 26.63 percent, 33.92 percent, 19 percent, per 1/4 wt % of titanium, zirconium and ti addition respectively in the present study. The weight percentage of titanium added was twice in the case of Misra with respect to the present observation for nearly the same initial fall of magnetic moment. Also, the initial dip and subsequent rise is more pronounced in the present work and it may be due to the better chemical homogenity of the dopant

5.2 LATTICE PARAMETER

The following are the observation of lattice parameter variation with the addition of high valent cations such as titanium, zirconium and tin in $Ni_{.3}Zn_{.7}Fe_2O_4$ in the present study.

1) The dip in lattice parameter was observed only in the case of titanium (Fig. 1). The dip is followed by a monotonic increase with higher additions of titanium.

2) The lattice parameter of zirconium and tin additions increases linearly as the ions presumably go into the solid solution (Fig. 1).

3) The peaks of monoclinic ZrO_2 phase were observed at higher percentages indicating the limited solubility of zirconium.

The observations of lattice parameter variation with similar high valent cation addition in Ni-Zn ferrite by earlier workers[8,25] are the following :

1) A dip in lattice parameter was observed upto 0.8 wt titanium substituted $Ni_{.5}Zn_{.5}Fe_2O_4$ followed by a monotonic rise by Das[8].

2) A dip in lattice parameter was observed by Misra[8] for

3) The linear increase of lattice parameter observed was followed by the flattening of the curve with zirconium, niobium additions in $Ni_{.5}Zn_{.5}Fe_2O_4$ showed the limit of their solubility in the case of Das[8].

There was no appropriate explanation given for the initial dip observed for titanium additions by Das. Misra's[8] explanation to the observed variation of lattice parameter of titanium substituted $Ni_{.3}Zn_{.7}Fe_2O_4$ was based on cation distribution resulting in an initial decrease of net charge at A site followed by a subsequent increase at later stage. From the analysis of cation distribution he concluded that

1) At very low percentages titanium enters the A site.
2) At higher percentages after a critical value, titanium starts entering the B site.
3) The entry of Ti^{4+} in the spinel lattice creates vacancies.

As a result, the charge at A site decreases with the entry of titanium, because of the combined effect of (a) excess charge of Ti^{4+} over one Fe^{3+} as it enters the site (b) transfer of same Fe^{3+} from A to B site and (c) removal of half divalent ion (zinc valency) from the site to maintain the charge balance

The lowering of charge at A site increases the Madelung constant (Gorter[2]) and the fact that the lattice parameter varies inversely with Madelung constant accounts for the initial dip. At higher percentages, Ti^{4+} starts entering the

B sites which increases the charge at A site leading to the increase in lattice parameter. Also, with higher additions of titanium, vacancies increase which tend to repel the neighbouring ions thereby causing further increase in the lattice parameter.

The explanation based on Misra fails to account the absence of initial dip in other qquativalent cations such as zirconium and tin (Fig. 1) additions in $Ni_{.3}Zn_{.7}Fe_2O_4$. The substitutions by zirconium and tin increases the lattice parameter as they presumably enter the solid solutions. The present observations of lattice parameter variation with zirconium addition are similar to that of Das[25].

In this case (Fig. 1) the limit of solubility of zirconium in $Ni_{.3}Zn_{.7}Fe_2O_4$ is 1 wt % , after which the linear increase of lattice parameter tends to flatten out. Also, peaks of ZrO_2 were observed at 3 and 8 wt % indicating the limited solubility of zirconium. Das[25] had found the solubility limit to be 3.40 wt % ZrO_2 in $Ni_{.5}Zn_{.5}Fe_2O_4$.

5.3 CURIE TEMPERATURE

The nature of the curves of magnetic moment variation with temperature in $Ni_{.3}Zn_{.7}Fe_2O_4$ improved with increase in firing time from 2 to 6 hours at $1200^{\circ}C$ (Fig. 5). This clearly indicates the improvement in homogenisation of the dopant in the ferrite matrix and better ferritisation of the material.

The dips in curie temperature with the dopant addition are observed in the additions of titanium, zirconium and tin (Figs. 7,8 and 9). The dips are followed by a rise in all the dopant additions, the rise being maximum in the case of titanium.

Gorter[2] showed that the substitutions of now magnetic ion in tetrahedral site cause a decrease in curie temperature and the substitution in octahedral site also decreases the curie temperature but relatively less. The addition of zinc ferrite to nickel ferrite decreases the curie point. Expression for determining the curie temperature of Ni-Zn ferrite was given by Gilleo[4] involving the interaction parameters. But to a system like ours no theoretical calculation of curie temperature is available. Misra[8] had indicated the possibility of determining the curie temperature using a 5-sublattice model. The working out of the problem will be an extensive theoretical works.

The observed variations of curie temperature with the quatrivalent cations like titanium, zirconium and tin are similar (Figs. 7,8 and 9). The initial fall and rise of curie temperature is more prominent in the case titanium than in zirconium and tin additions. The observed variation is not understood in any of the above high-valent cation addition in $Ni_{.3}Zn_{.7}Fe_2O_4$.

The temperature variation of magnetic moment of the titanium, zirconium, and tin add tions is shown in Figs. 4,5 and 6. In all the cases the magnetic moment does not become zero and a small tail is observed near the curie point. Our method of sample preparation is expected to be more chemically homogenous and this tail cannot be attributed to chemical inhomogenity alone. Further interpretation in terms of short-range ordering is required to explain the observed tail. However, no further analysis of the tail was carried out and curie temperature was determined from $\frac{d\sigma}{dT}$ versus T curves.

SUMMARY AND CONCLUSIONS

$Ni_{.3}Zn_{.7}Fe_2O_4$ was doped with titanium, zirconium and tin by the solution method to a limit of 8 wt %, 8 wt % and 5 wt % respectively.

Step-scan method in conjunction with X-ray diffractometer was used for lattice parameter determination. The accurate extrapolated lattice parameter values were calculated from the lattice parameter versus Nelson-Riley function plot by least square fit of a straight line.

Vibrating magnetometer was used to determine the saturation magnetisation at 10KOe and the curie temperature at a residual field of 40 Oe.

For Ti^{4+} doped samples, the lattice parameter drops sharply at low percentages followed by a monotonic rise upto 8 wt %. This may be explained on the basis of increase in charge due to the entry of Ti^{4+} ions in the A sites at low percentages. The entry of Ti^{4+} ions to B sites at higher percentages decreases the net-charge at A site and also the number of vacancies increase thereby further increasing the lattice parameter.

The lattice parameter of Zr^{4+} ions doped samples increases upto 1 wt % and then tends to flatten off indicating the limit of solubility of zirconium. The lattice parameter of Sn^{4+} increases monotonically upto the limit of the study. The lattice parameter increase in both Zr^{4+} and Sn^{4+} ions is explained on the basis of cation vacancies.

Sharp initial decrease of magnetic moment is observed with the additions of Ti^{4+}, Zr^{4+}, and Sn^{4+}. In the case of titanium addition the initial dip is followed by subsequent ris and again a fall in magnetic moment at higher percentages. In the case of zirconium addition the initial dip is followed by a gradual slope and a very small increase and with tin addition the initial dip is followed by a gradual change of slope.

The observed variations of magnetic moment in all the thre cation additions may be explained based on the model of transfe process of Fe^{3+} ions depending on the site preference of the substituting ion.

With the addition of titanium, zirconium and tin the curie temperature falls steeply at low percentages, followed by subsequent rise. This is maximum in the case of titanium. These observations could not be explained for any of the dopant addition although a similar variation has been observed earlier.

The refiring and regrinding of the samples improved the relative sharpness of the transition of magnetic moment with temperature. The samples fired for 6 hours with regrinding showed a relatively sharper transition indicating the better homogenity.

Table 1

Ionic radii and atomic weights of component elements*

Elements	Atomic weight	Normal valency state*	Ionic radius (°A)
Nickel (Ni)	58.71	2^+	0.69
Zinic (Zn)	65.37	2^+	0.74
Iron (Fe)	55.85	2^+ 3^+	0.64
Titanium (Ti)	47.90	4^+	0.68
Zirconium (Zr)	91.22	4^+	0.79
Tin (Sn)	118.69	4^+	0.71

*Reference : - 'Hand Book of Chemistry and Physics', CRC Press, both edition, 1980-81, p. F-214.

Table 2

Batch composition

1) Packing material

Component	Molecular weight	Composition (parts)	Percentage weight of the component	Grade
NiO	74.71	15	9.375	L.R.
ZnO	81.37	35	23.825	L.R.
Fe$_2$O$_3$	159.70	50	66.800	L.R.

ii) Base-ferrite (Ni$_{.3}$Zn$_{.7}$Fe$_2$O$_4$)

Metal	Atomic weight	Percentage weight of the metal	Metal oxide formed	Percentage weight of metal oxide formed
Nickel	58.71	10.06	NiO	9.37
Zinc	65.37	26.14	ZnO	23.83
Iron	55.85	63.80	Fe$_2$O$_3$	66.80

2	3	4	5	6	7
0.0075	0.25	0.0282	3.40	90.00	
0.0150	0.50	0.0564	6.80	90.00	
0.0300	1.00	0.1128	13.55	90.00	0.1255
0.0450	1.50	0.1693	20.30	90.00	
0.0900	3.00	0.3385	40.60	90.00	
0.2390	8.00	0.9027	108.30	90.00	

tum

0.0049	0.23	0.0250	2.20	59.90	0.1655
0.0097	0.50	0.0500	4.40	59.75	
Zirconium 0.0194	1.00	0.1000	8.80	59.45	
0.0291	1.50	0.1500	13.20	59.15	
0.0582	3.00	0.3000	26.25	58.25	
0.1550	8.00	0.8000	70.00	55.25	
0.0040	0.25	0.0250	1.25	59.90	
0.0080	0.50	0.0500	2.50	59.75	
Tin 0.0160	1.00	0.1000	5.00	59.45	0.1655
0.0320	2.00	0.2000	10.00	58.85	
0.0800	5.00	0.5000	25.00	57.05	

Tabl 4

X-ray diffraction lines $Ni_{.3}Zn_{.7}Fe_2O_4$ compared with ASTM data

ASTM X-ray hkl	data for Ni-Zn ferrite d A°	Observed dispacing for $Ni_{.3}Zn_{.7}Fe_2O_4$
111	4.85	—
220	2.966	2.985
211	2.699	—
311	2.533	2.535
222	2.423	2.424
400	2.100	2.100
422	1.715	1.718
511,333	1.617	1.619
440	1.485	1.490
531	1.417	—
620	1.327	1.328
583	1.280	1.283
444	1.212	—
551,711	1.174	—
642	1.122	—
553,731	1.093	—
800	1.043	—

X-ray unit = Seifert (Germany)
Target = Cromium
Scan speed = 3°min.
Chart speed 15°/min.

mole fraction	2θ (degrees)	θ (degrees)	d (A°)	hkl	Lattice parameter for different d values (A°)	Nelson-Riley functions f(θ)	Slope	Extrapolated value of lattice parameter (A°)
2	3	4	5	6	7	8	9	10
	45.370	22.685	2.9702	220	8.4010	2.8804		
	3.720	26.860	2.5354	311	8.4088	1.9041		
	55.350	28.175	2.4260	222	8.4041	1.7565		
	66.100	33.050	2.1004	400	8.4016	1.1917	−0.0061	8.4178
	83.580	41.790	1.7189	422	8.4210	0.6325		
	90.000	45.000	1.6200	511	8.4176	0.5056		
	100.480	50.240	1.4901	440	8.4294	0.3502		
	119.130	59.565	1.3286	620	8.4025	0.1247		
	126.400	63.200	1.2834	533	8.4155	0.1292		

0.25	0.0075	45.375	22.687	2.9699	220	8.4001	2.8797		
		53.775	26.387	2.5330	311	8.4008	1.9595		
		56.400	28.200	2.4241	222	8.3973	1.7529		
		66.060	33.030	2.1015	400	8.4061	1.1935	−0.0056	8.4127
		83.735	41.867	1.7163	422	8.4083	0.6291		
		90.090	45.045	1.6187	511	8.4111	0.5038		
		100.750	50.375	1.4872	440	8.4129	0.3468		
		119.050	59.525	1.3291	620	8.4061	0.1753		
		126.350	63.175	1.2836	533	8.4174	0.1295		
0.50	0.0150	45.315	22.657	2.9736	220	8.4107	2.8882		
		53.710	26.855	2.5358	311	8.4103	1.9650		
		56.235	28.117	2.4306	222	8.4199	1.7650		
		66.050	33.025	2.1018	400	8.4073	1.1940	−0.0019	8.4160
		83.685	41.842	1.7171	422	8.4124	0.6302		
		90.030	45.015	1.6197	511	8.4155	0.5050		
		100.725	50.362	1.4875	440	8.4145	0.3471		
		118.765	59.382	1.3311	620	8.4184	0.1773		
		126.350	63.175	1.2836	533	8.4174	0.1295		

45.350	22.675	2.9714	220	8.4045	2.8832		
53.775	26.887	2.5330	311	8.4008	1.9595		
56.300	28.150	2.4280	222	8.4110	1.7602		
66.020	33.010	2.1027	400	8.4107	1.1953		
83.750	41.875	1.7161	422	8.4071	0.6288	-0.0046	8.41..
90.100	45.050	1.6186	511	8.4103	0.5038		
100.790	50.395	1.4869	440	8.4105	0.3463		
118.950	59.475	1.3298	620	8.4104	0.1760		
126.070	63.035	1.2852	533	8.4278	0.1310		

1.00 0.0300

45.430	22.715	2.9665	220	8.3905	2.8720		
53.815	26.907	2.5312	311	8.3951	1.9562		
56.330	28.165	2.4268	222	8.4068	1.7580		
66.050	33.025	2.1018	400	8.4073	1.1940	-0.0087	8.4162
83.740	41.870	1.7163	422	8.4079	0.6290		
90.100	45.050	1.6186	511	8.4103	0.5038		
100.790	50.395	1.4868	440	8.4105	0.3463		
118.815	59.407	1.3307	620	8.4163	0.1770		
126.350	63.175	1.2836	533	8.4174	0.1295		

1.50 0.0450

3.00 **0.0900**							
45.350	22.675	2.9714	220	8.4045	2.8832		
53.750	26.875	2.5340	311	8.4045	1.9616		
65.965	32.982	2.1042	400	8.4169	1.1978		
83.670	41.835	1.7174	422	8.4136	0.6306	-0.0049	8.4178
90.050	45.025	1.6193	511	8.4140	0.5047		
100.700	50.350	1.4878	440	8.4160	0.3475		
118.800	59.400	1.3308	620	8.4170	0.1771		
126.350	63.175	1.2836	533	8.4174	0.1295		
8.00 **0.2390**							
45.300	22.650	2.9746	220	8.4133	2.8903		
53.670	26.835	2.5375	311	8.4161	1.9684		
56.250	28.125	2.4300	222	8.4178	1.7639		
65.950	32.975	2.1046	400	8.4186	1.1985		
83.600	41.800	1.7186	422	8.4194	0.6321	-0.0023	8.4205
90.010	45.005	1.6199	511	8.4170	0.5054		
100.650	50.325	1.4883	440	8.4190	0.3481		
118.665	59.332	1.3318	620	8.4228	0.1780		
126.300	63.150	1.2839	533	8.4192	0.1298		

1	2	3 (de-grees)	4 (de-grees)	5 (A°)	6	7 parameter for different d values (A°)	8 Riley function f(θ)	9	10 calculated value of lattice parameter (A°)
		45.380	22.690	2.9696	220	8.3992	2.8790		
		53.740	26.870	2.5345	311	8.4057	1.9625		
		56.330	28.165	2.4268	222	8.4068	1.7580		
		66.040	33.020	2.1021	400	8.4084	1.1944		
0.25	0.0049	83.660	41.830	1.7176	422	8.4145	0.6308	−0.0066	8.4183
		90.035	45.017	1.6195	511	8.4151	0.5049		
		100.700	50.350	1.4877	440	8.4160	0.3475		
		118.800	59.400	1.3308	620	8.4169	0.1771		
		126.335	63.167	1.2837	533	8.4179	0.1296		

.50 0.0097

45.315	22.657	2.9736	220	8.4107	2.8882
53.685	26.842	2.5369	311	8.4139	1.9672
56.290	28.145	2.4284	222	8.4123	1.7610
65.990	32.995	2.1035	400	8.4141	1.1967
83.630	41.815	1.7181	422	8.4169	0.6314
89.980	44.990	1.6203	511	8.4192	0.5059
100.650	50.325	1.4883	440	8.4190	0.3480
118.755	59.377	1.3311	620	8.4189	0.1774
126.300	63.150	1.2839	533	8.4192	0.1298

-0.0033 8.4196

1.00 0.0194

45.300	22.650	2.9746	220	8.4133	2.8903
53.675	26.837	2.5373	311	8.4153	1.9680
56.250	28.125	2.4300	222	8.4178	1.7639
65.955	32.977	2.1045	400	8.4180	1.1983
83.615	41.807	1.7183	422	8.4181	0.6318
89.920	44.960	1.6211	511	8.4236	0.5070
100.640	50.320	1.4884	440	8.4196	0.3482
118.690	59.345	1.3316	620	8.4217	0.1778
126.300	63.150	1.2839	533	8.4192	0.1298

-0.0027 8.4214

45.300	22.650	2.9746	220	8.4133	2.8903		
53.670	26.835	2.5375	311	8.4160	1.9684		
56.265	28.132	2.4294	222	8.4158	1.7628		
65.960	32.980	2.1044	400	8.4175	1.1981		
83.620	41.810	1.7183	422	8.4177	0.6317	−0.0024	8.4203
89.975	44.987	1.6203	511	8.4195	0.5060		
100.635	50.317	1.4884	440	8.4199	0.3483		
118.730	59.365	1.3313	620	8.4200	0.1776		
126.285	63.142	1.2840	533	8.4198	0.1298		

0.0291

45.380	22.690	2.9696	220	8.3992	2.8790		
53.820	26.910	2.5310	311	8.3943	1.9557		
56.370	28.185	2.4253	222	8.4014	1.7551		
66.085	33.042	2.1008	400	8.4033	1.1924		
83.770	41.885	1.7158	422	8.4054	0.6284	−0.0056	8.4108
90.145	45.072	1.6179	511	8.4071	0.5030		
100.865	50.432	1.4860	440	8.4060	0.3454		
119.050	59.525	1.3291	620	8.4061	0.1753		
126.760	63.125	1.2842	533	8.4211	0.1300		

0.0582

	45.310	22.655	2.9739	220	8.4115	2.8889	
	53.700	26.850	2.5362	311	8.4117	1.9659	
	56.285	28.142	2.4286	222	8.4130	1.7613	
	65.980	32.990	2.1038	400	8.4152	1.1972	−0.0023	8.4179
	83.650	41.825	1.7178	422	8.4153	0.6310	
	89.960	44.980	1.6206	511	8.4206	0.5063	
	100.680	50.340	1.4880	440	8.4172	0.3477	
	118.785	59.392	1.3309	620	8.4176	0.1772	
8.00 0.1550	126.400	63.200	1.2833	533	8.4155	0.1292	

wt %	Mole-fraction	2θ (degrees)	θ (degree)	d (Å)	hkl	Lattice parameters for different d-values (Å)	Nelson-Riley function f(θ)	Slope	Extrapolated value of lattice parameter (Å)
1	2	3	4	5	6	7	8	9	10
		45.275	23.637	2.9761	220	8.4177	2.8938		
		53.675	26.837	2.5373	311	8.4153	1.9680		
		56.250	28.125	2.4300	222	8.4178	1.7639		
		65.950	32.975	2.1046	400	8.4185	1.1985		
0.25	0.0040	83.590	41.795	1.7188	422	8.4202	0.6323	-0.0020	8.4215
		89.945	44.972	1.6208	511	8.4217	0.5065		
		100.615	50.307	1.4887	440	8.4212	0.3485		
		118.725	59.362	1.3313	620	8.4202	0.1776		
		126.215	63.107	1.2844	533	8.4223	0.1302		

0.0080	45.340	22.670	2.9720	220	8.4063	2.9846	
	53.715	26.857	2.5356	311	8.4095	1.9646	
	56.275	28.137	2.4290	222	8.4144	1.7620	
	65.995	32.997	2.1033	400	8.4135	1.1964	
	83.595	41.797	1.7187	422	8.4198	0.6322	
	89.960	44.980	1.6207	511	8.4206	0.5063	
	100.640	50.320	1.4884	440	8.4196	0.3482	
	118.650	59.325	1.3319	620	8.4234	0.1781	−0.0062 8.4215
	126.200	63.100	1.2845	533	8.4229	0.1303	
0.0160	45.285	22.642	2.9755	220	8.4159	2.8924	
	53.630	21.815	2.5393	311	8.4218	1.9718	
	56.220	28.110	2.4312	222	8.4219	1.7661	
	65.950	32.975	2.4046	400	8.4186	1.1985	
	83.430	41.715	1.7214	422	8.4334	0.6359	
	89.870	44.935	1.6218	511	8.4273	0.5079	
	100.525	50.262	1.4896	440	8.4267	0.3496	
	118.570	59.285	1.3324	620	8.4269	0.1787	−0.0042 8.4287
	126.130	63.065	1.2848	533	8.4256	0.1307	

45.325	23.662	2.9729	220	8.4089	2.8868		
53.280	26.840	2.5371	311	8.4146	1.9676		
56.270	28.135	2.4292	222	8.4150	1.7624		
65.960	32.980	2.1043	400	8.4174	1.1981		
83.560	41.780	1.7192	422	8.4227	0.6330	-0.0074	8.4288
89.885	44.942	1.6216	511	8.4261	0.5076		
100.500	50.250	1.4899	440	8.4282	0.3499		
118.610	59.305	1.3321	620	8.4252	0.1784		
126.000	63.000	1.2856	533	8.4304	0.1314		
45.215	22.607	2.9798	220	8.4283	2.9024		
53.700	26.850	2.5362	311	8.4117	1.9659		
56.160	28.080	2.4336	222	8.4302	1.7706		
65.820	32.910	2.1083	400	8.4333	1.2045		
83.400	41.700	1.7219	422	8.4358	0.6365	-0.0055	8.4376
89.750	44.875	1.6235	511	8.4361	0.5100		
100.300	50.150	1.4920	440	8.4404	0.3524		
118.350	59.175	1.3339	622	8.4366	0.1803		
125.950	62.975	1.2859	533	8.4323	0.1317		

0.0320

0.0800

.00

5.00

Table 8

Variation of magnetic moment of $Ni_{.3}Zn_{.7}Fe_2O_4$ with
applied field at room temperature

pplied field (K. Oe)	Magnetic moment	
.00	0.0007	0.098
.1	0.0546	7.668
.3	0.1570	22.050
.5	0.2360	33.146
.7	0.2920	41.011
.0	0.3440	48.314
.0	0.3970	55.758
.0	0.4110	57.724
.0	0.4190	58.848
.0	0.4240	59.550
.0	0.4280	60.112
.0	0.4310	60.533
.0	0.4340	60.955
.0	0.4370	61.376
0.0	0.4390	61.657

oom temperature $= 24^{o}C$

ass of the sample $= 0.0712$ gms.

Table 9

Saturations magnetic moment, curie temperature and lattice parameter of $Ni_{.3}Zn_{.7}Fe_2O_4$ with different dopants

Dopant	wt% of the dopant	More of the dopant	Saturation magnetisation (emu/gm)	$4\pi M$ (Gauss)	Curie temperature (°C)	Lattice parameter (Å)
1	2	3	4	5	6	7
-	-	-	61.657	4125.1	201.1	8.4178
	0.25	0.0075	45.317	3031.9	129.8	8.4127
	0.50	0.0150	40.873	2734.5	112.8	8.4160
	1.00	0.0300	44.046	2946.8	167.2	8.4153
Titanium	1.50	0.0450	53.953	3609.6	188.2	8.4162
	3.00	0.0900	48.168	3222.6	166.0	8.4178
	8.00	0.2390	28.961	1937.6	123.2	8.4205

Zirconium	0.25	0.0049	40.746	2726.0	101.4	8.4183
	0.50	0.0097	39.367	2633.8	112.4	8.4196
	1.00	0.0194	38.666	2586.9	110.0	8.4203
	1.50	0.0291	39.575	2647.7	109.8	8.4203
	3.00	0.0582	44.854	3000.9	216.8	8.4108
	8.00	0.1550	42.325	2831.7	144.9	8.4179
Tin	0.25	0.0040	49.944	3341.4	107.0	8.4215
	0.50	0.0080	45.911	3071.6	113.8	8.4232
	1.00	0.0160	44.690	2989.9	95.9	8.4287
	2.00	0.0320	43.478	2908.8	110.9	8.4288
	5.00	0.0800	43.120	2884.9	113.9	8.4375

Lattice parameter in Å

Residual field = 40 Oe
● 2 hours
▲ 4 hours
○ 6 hours

(y-axis) Tc Moment in emu/gm

(x-axis) Temperature (°C)
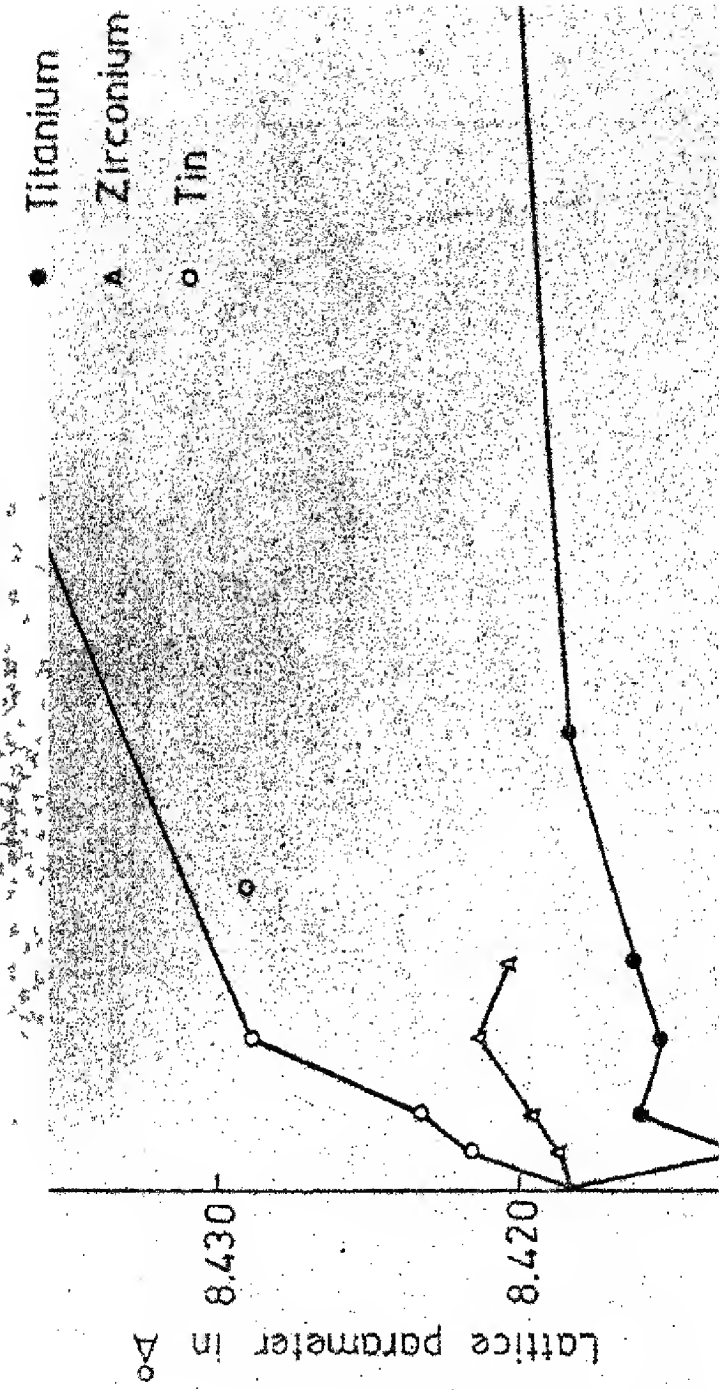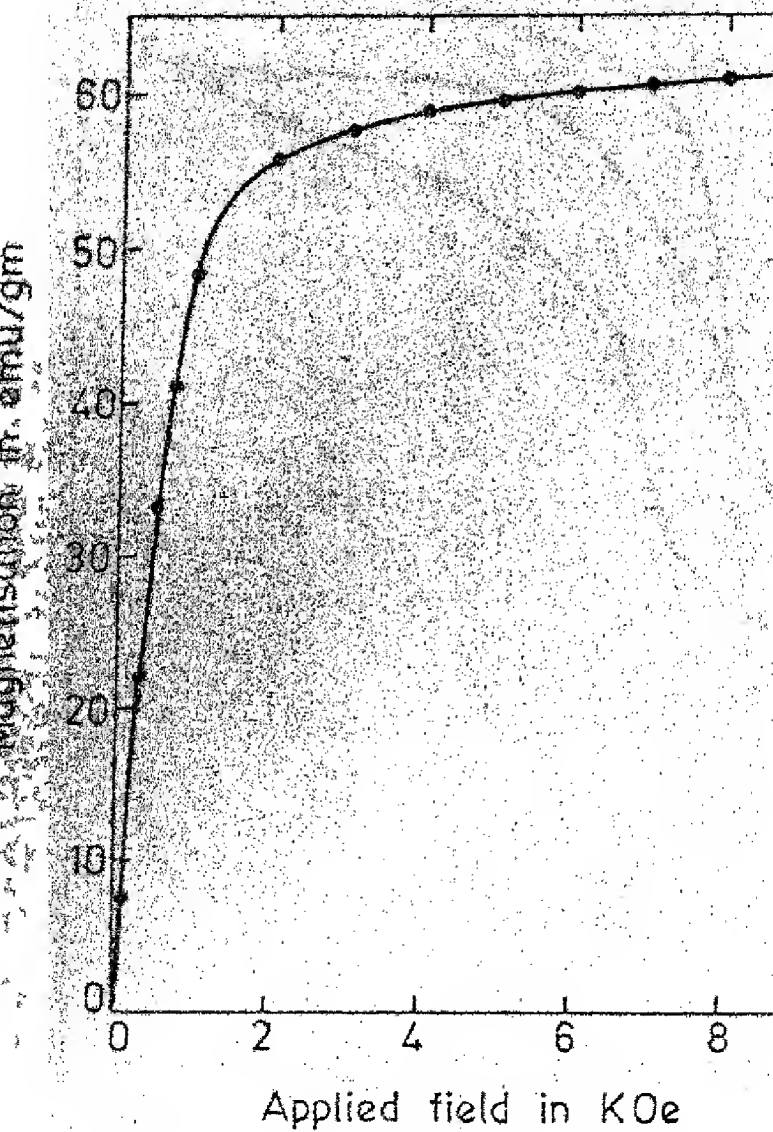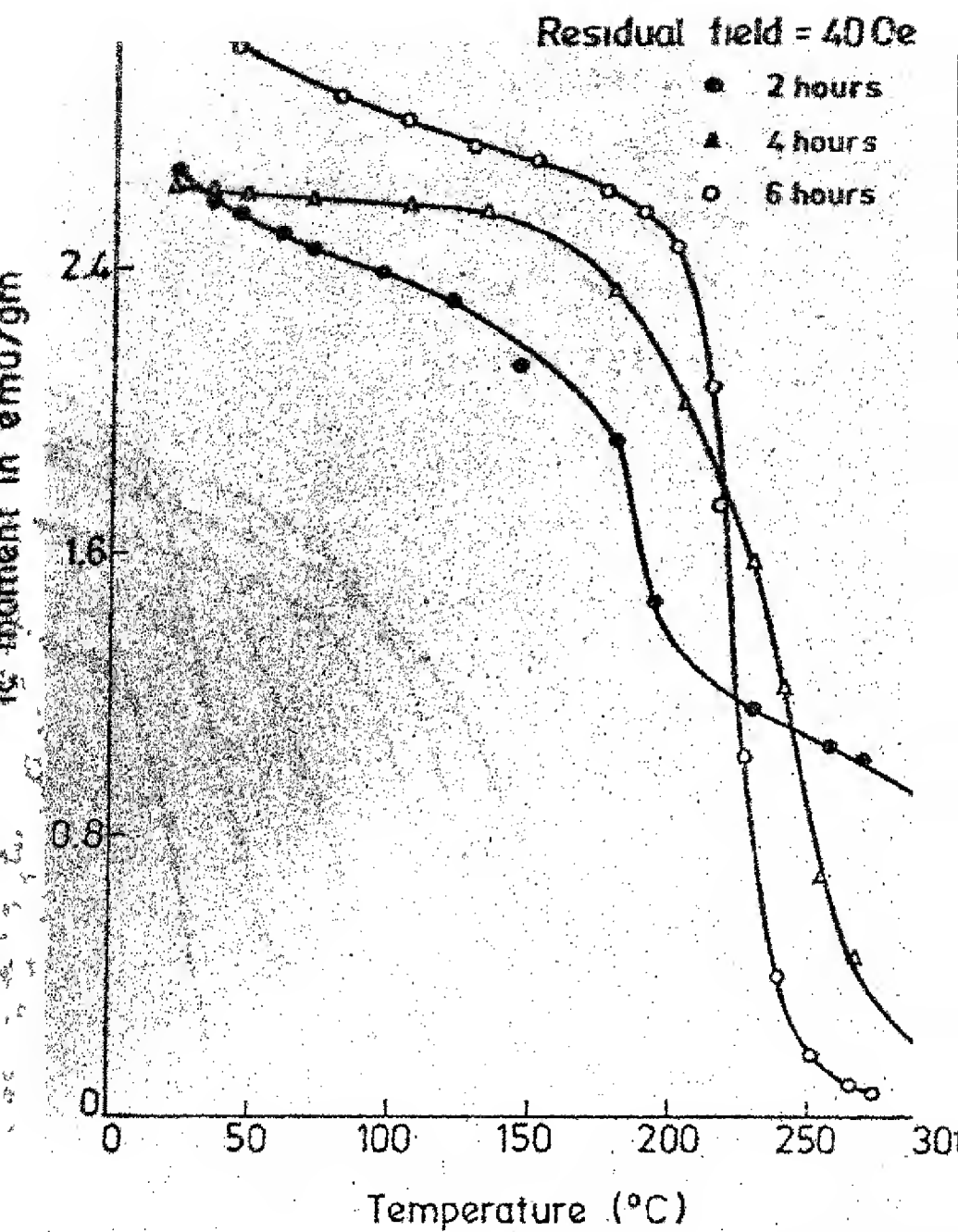
Residual field = 40 O

▲	0.25 wt%
○	0.50 wt%
▢	1.00 wt%
●	1.50 wt%
▲	3.00 wt%
■	8.00 wt%

Temperature (°C)
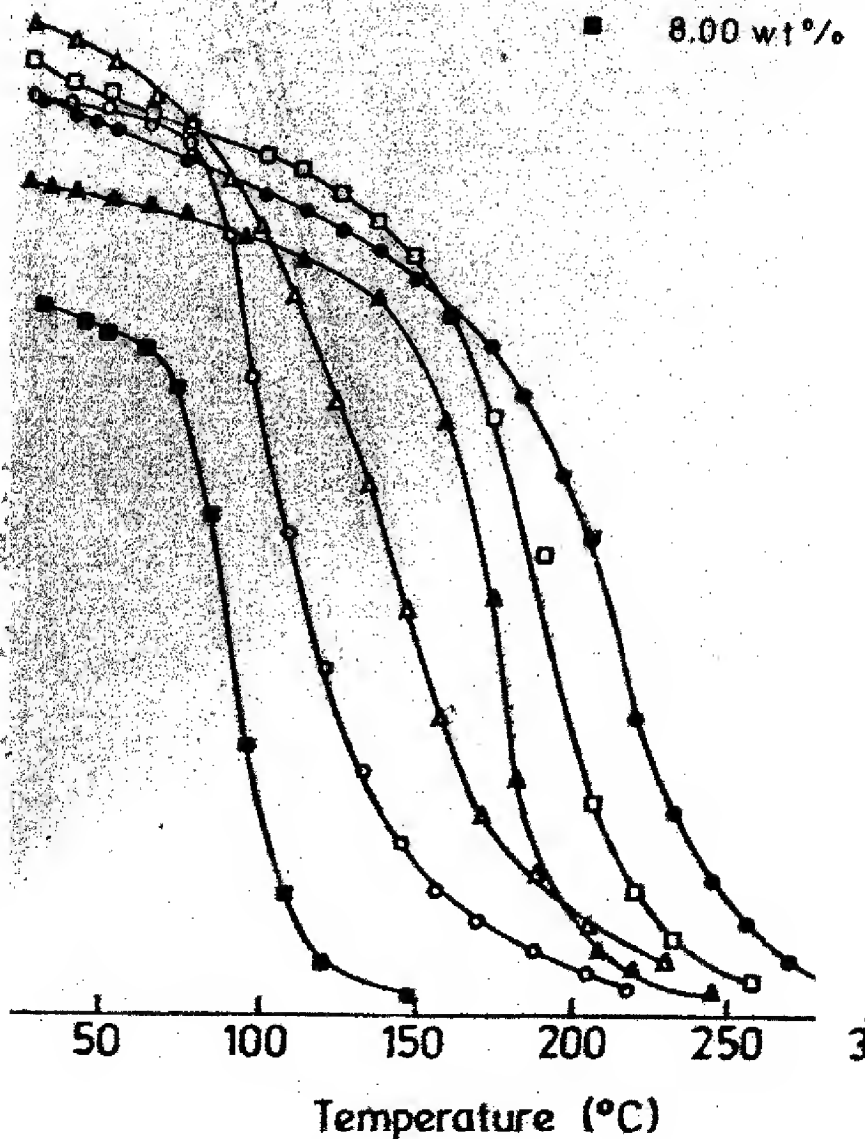
Residual field = 40 O

△	0.25 wt %
○	0.50 wt %
▫	1.00 wt %
●	1.50 wt %
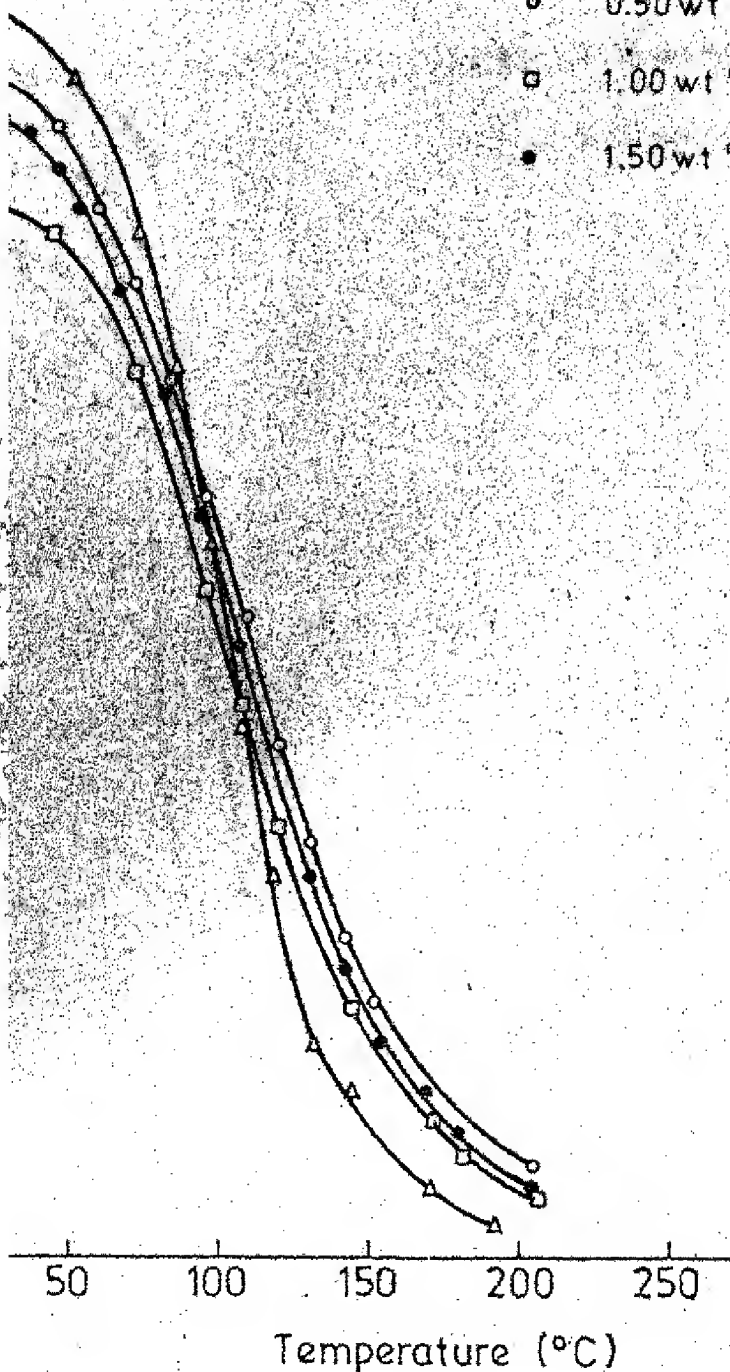
Temperature (°C)

Residual field = 40 Oe

△	0.25 wt %
○	0.50 wt %
▢	1.00 wt %
▲	2.00 wt %
●	5.00 wt %

Temperature (°C)

Magnetic moment

Curie temperature
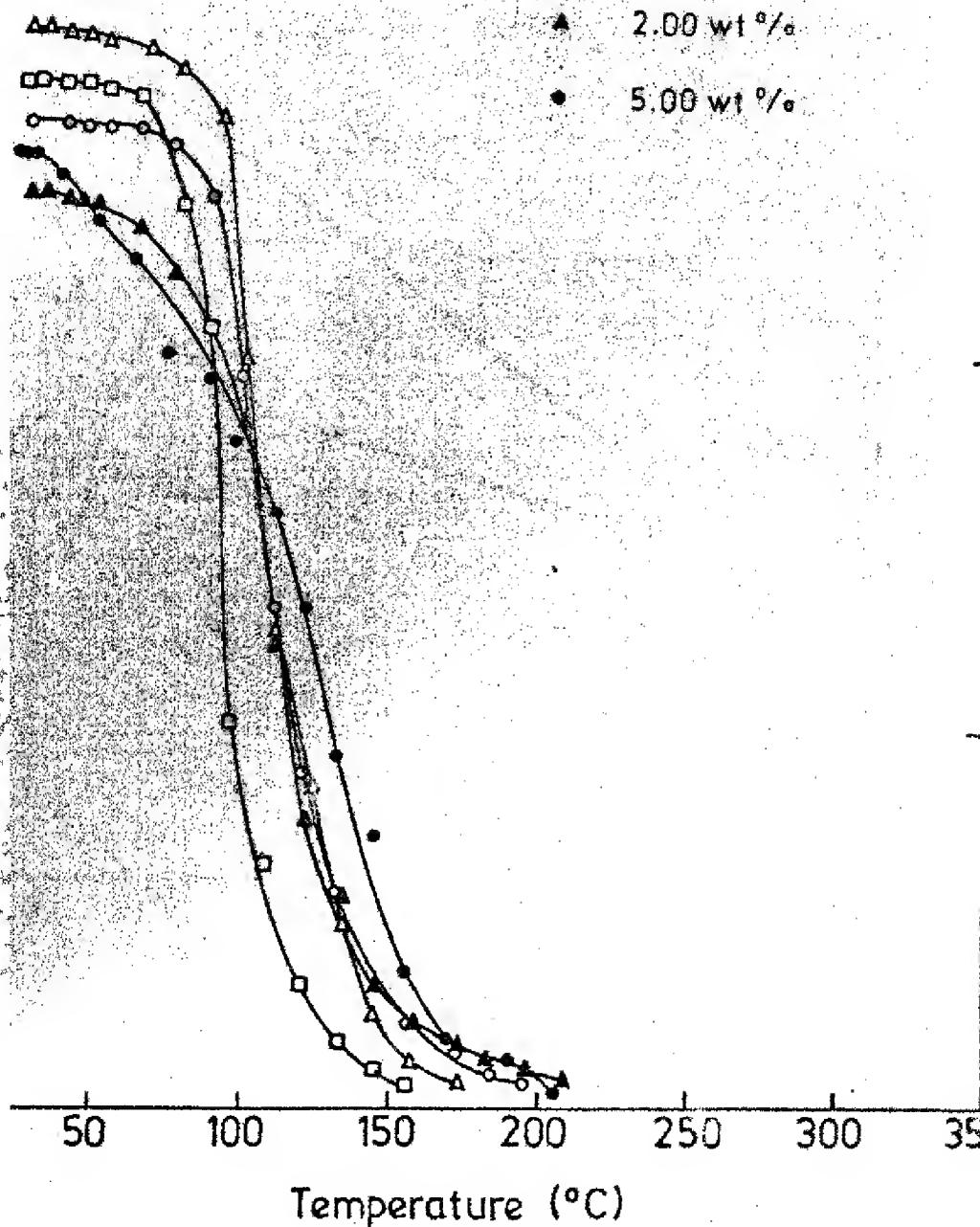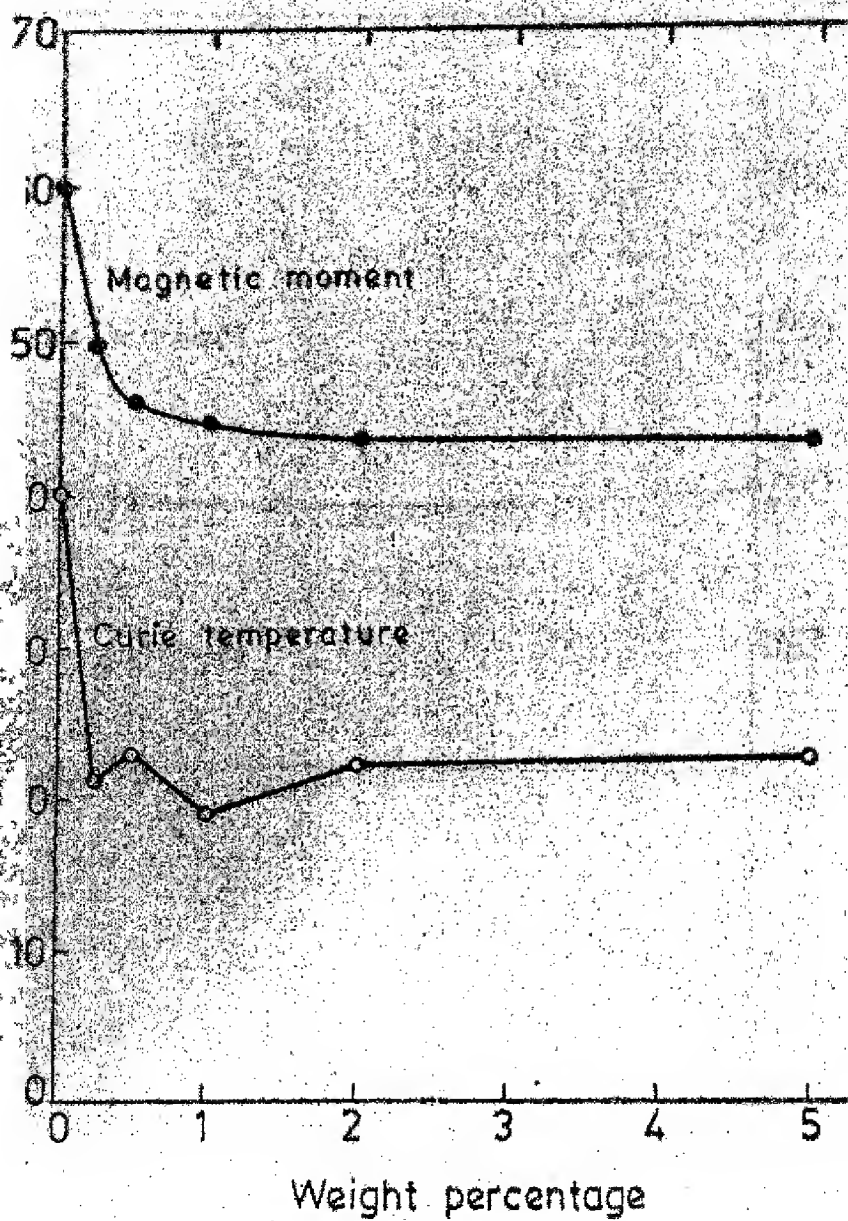
Weight percentage

magnetic moment

temperature

0.5   1.0   1.5

Weight percentage

Snoek, 'Non metallic magnetic materials for high
uency', Philips Tech. Review, 8 (1946), pp. 353-360.
Gorter, 'Saturation magnetisation and crystal
istry of ferrimagnetic oxides', Philips Res. Rep. 9
4), pp. 403-443.
lasse, 'Crystal chemistry and some magnetic properti
ixed metal oxides with spinel structure', Philips
Rep., 1953, (1964).
Gilleo, 'Super exchange interactions in ferrimagnet
ets and spinels which contain randomly incomplete
ages', J.Phy. Chem. Solids, Pregamon Press, vol. 13
8), pp. 33-39.
Swant and R.N. Patil, 'Cation distribution from
e temperature of Cu-Zn ferrite', Indian J. Pure. App
ics, 19 (12), 1981, pp. 1212-13.
rose van Groenou, B.F. Bongers and A.L. Stuyts,
netism, microstructure and crystal chemistry of
el ferrites', Material Sci. Engg., 3 (1968-69),
319-331.
.Satyamurthy, M.G. Nateria, S.I. Yousseff,
. Begum and C.M. Sreevastava, Phy.Rev., 81 (1969),
969.

Misra, 'Magnetic studies of titanium substitut
.7 - Ferrites and some alloy systems', Ph.D. Th
Kanpur (1981).

rivastava, G. Srinivasan and N.G. Nandikar,
-Kittel angles in zinc-nickel ferrites, Phys.
19 (1979), p. 499.

nowles, 'Magnetic after effects in ferrites
ituted with Ti or Sn', Philips Res. Rep. 29
), p. 93.

es et al., 'Permeability and conductivity of Ti
ituted Mn-Zn ferrite', Philips Res.Rep. 25 (2),
, p. 95.

upta and A.R. Das, 'Effect of processing parame-
crostructure development and magnetic spectrum o
.7 Fe2O4 ferrite; 1 - Ferritisation and micro-
ture development', Trans. Indian Ceramic Soc., 3
pp. 47-55.

Brockman and K.E. Matteson, 'New techniques for
se control of stoichometry of Ni-Zn ferrites',
nted in 71st annual meeting of Amer. Cera. Soc.,
act given in 'Amer. Cera.Soc. Bull. 48 (4), (196
0.

Slick and H. Blassches, 'Thermo gravimetric stud
gas interactions of Mn-Zn ferrite and effect on
tic properties', IEEE Trans. (Magnetics), MAG-2,
, pp. 603 607.

'an'kov and L.A. Bashkirov, 'Mechanism of Ni-Zn

te formation', J. Solid State Chem., (USA),

, 1981, pp. 298-308.

T. Dimova, 'Spinel formation in Ni-Zn ferrites',

keram (zech), 32 (8), (1982), pp. 207-9,

cal Abs ., vol. 97, No.24, (1982).

it and H.P.J. Wijn, 'Ferrites', Philips technical

ry, Eindhoven (Holland), (1958), p. 145.

Powder diffraction file No. 8-234.

nit and H.P.J. Wijn, 'Ferrites', Philips Technical

ary, Eindhoven (Holland), (1958), p. 158.

Parkins, 'Metlons modern inorganic chemistry',

mans, p. 876.

d Book of Chemistry and Physics', CRC Press Inc.,

or Robert C. Wart.

yclopedia of chemical reactions', compiled by

. Jacobson and edited by Clifford A. Hampell, VI-3

fred W. Scott, 'Standard methods of chemical analys

Van Nostrand Company, Inc., Vol. 1 - The elements,

978.

cyclopedia of chemical reactions', compiled by C.A

obson and edited by Cliff A. Hampell, VII-984,

II-985.

. Das, 'M.Tech. Thesis', IIT Kanpur, (1981).

26. P.K. Das and A.R. Das, 'Effect of titanium, zirconium,
     and niobium on lattice parameters, density and satura-
     tion moment of $Ni_{.5}Zn_{.5}Fe_2O_4$', to be published in
     Trans. Indian Cera. Soc.

27. A.R. Das and A. Sen, 'Effect of TiO_2 additions on
     saturation magnetisation and magnetic spectrum of
     $Ni_{.3}Zn_{.7}Fe_2O_4$ ferrite', Trans. of Indian. Cera.Soc.,
     40 (4), (1981).

28. Yafet, Y. and Kittel, C., 'Antiferromagnetic arrangements
     in ferrites', Phy. Rev., 87 (2), (1952) pp. 290-94.

APPENDIX

ESTIMATION OF LATTICE PARAMETER

The lattice parameter was precisely estimated using Nelson-Riley function.

The d values were calculated using Bragg's law

$$\lambda = 2d \sin\theta$$

where '2θ' was the diffraction angle and ' ' was the wavelength of chromium K_α target.

The d-values calculated were used to find out the lattice parameter, 'a' as

$$a = d(h^2+k^2+l^2)^{\frac{1}{2}}$$

where hkl were the indices for the diffracting planes adopted from ASTM data file for Ni-Zn ferrite.

Precise lattice parameter was obtained by extrapolating the lattice parameter to $\theta = 90^{\circ}$ and using Nelson-Riley extrapolation function $f(\theta)$. This function was chosen to use the low angle reflections for extrapolation of the lattice parameters. The Nelson-Riley function is given by

$$f(\theta) = (\frac{\cos^2\theta}{\sin\theta} + \frac{\cos^2\theta}{\theta})$$

Accurate determination of angle was done by step scan method. The X-ray counts were plotted against 2θ. The curves for 1 wt %, titanium substituted $Ni_{.3}Zn_{.7}Fe_2O_4$ are shown in Fig. 10. The exact 2θ corresponds to the maximum peak position which was measured accurately upto ± 0.01 degree.

A computer program was written to calculate the extrapolated lattice parameter from the lattice parameter versus Nelson-Riley function plot by least square fit of a straight line. The calculated d, hkl, lattice parameters and the corresponding Nelson-Riley function are given in Tables 5,6 and 7. The extrapolated lattice parameters are given in Tables 5,6,7 and 9, for titanium, zirconium and tin additions in $Ni_{.3}Zn_{.7}Fe_2O_4$.
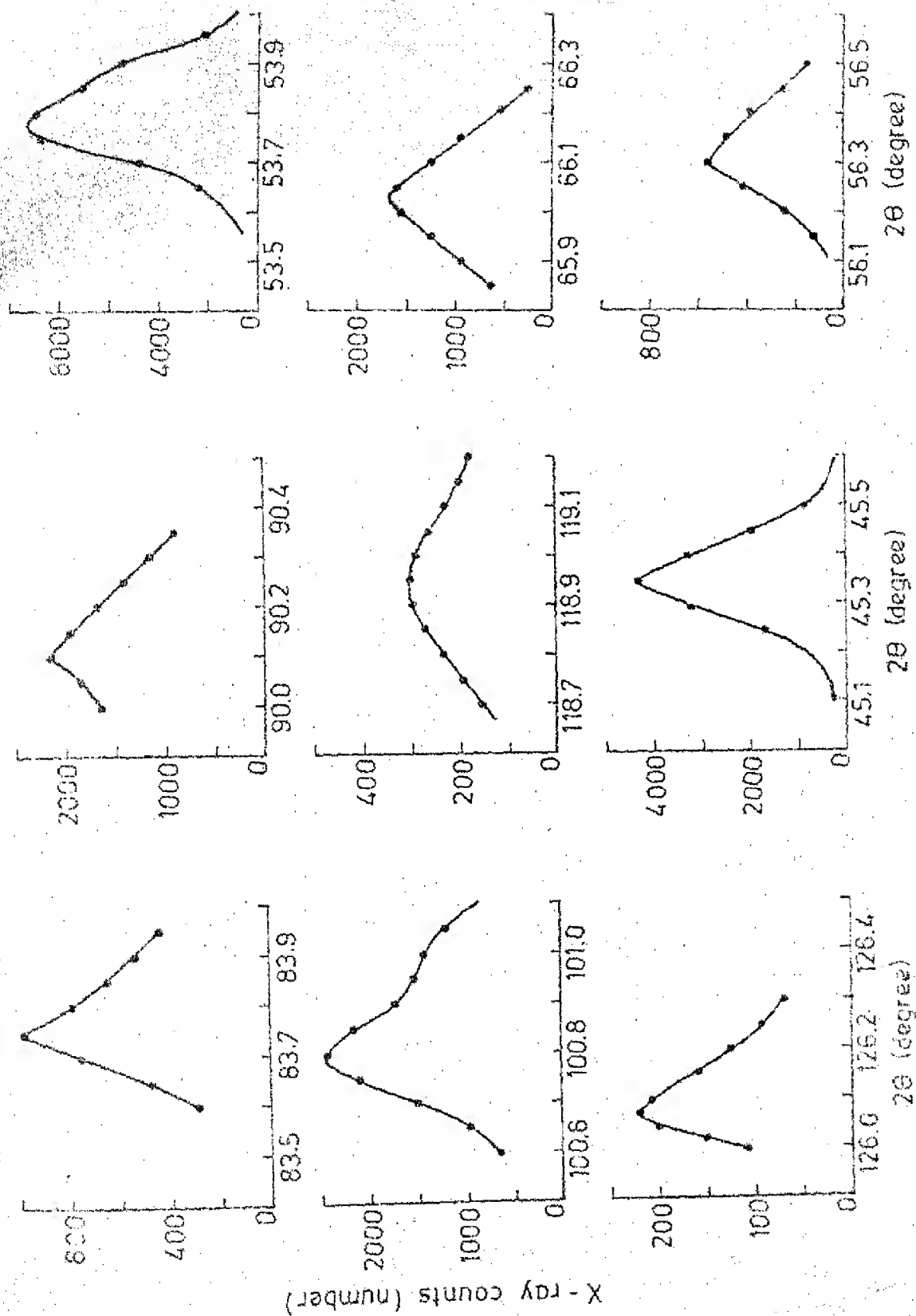
Variation of X-ray counts with angle (2θ) for 1% of titanium doped $Ni_{0.3}Zn_{0.7}Fe_2O_4$.